A NUMERICALLY RESEARCH ON ENERGY LOSS EVALUATION IN A CENTRIFUGAL PUMP SYSTEM BASED ON LOCAL ENTROPY PRODUCTION METHOD

by

Hucan HOU Yongxue ZHANG*[*] Zhenlin LI

College of Mechanical and Transportation Engineering, China University of Petroleum-Beijing, Beijing 102249, China
Beijing Key Laboratory of Process Fluid Filtration and Separation, China University of Petroleum-Beijing, Beijing 102249, China

Inspired by wide application of the second law of thermodynamics to flow and heat transfer devices, local entropy production analysis method was creatively introduced into energy assessment system of centrifugal water pump. Based on Reynolds stress turbulent model and energy equation model, the steady numerical simulation of the whole flow passage of one IS centrifugal pump was carried out. The local entropy production terms were calculated by user defined functions, mainly including wall entropy production, turbulent entropy production and viscous entropy production. The numerical results indicated that the irreversible energy loss calculated by the local entropy production method agreed well with that calculated by the traditional method but with some deviations which were probably caused by high rotatability and high curvature of impeller and volute. The wall entropy production and turbulent entropy production took up large part of the whole entropy production about 48.61% and 47.91% respectively, which indicated that wall friction and turbulent fluctuation were the major factors in affecting irreversible energy loss. Meanwhile, the entropy production rate distribution was discussed and compared with turbulent kinetic energy dissipation rate distribution, it showed that turbulent entropy production rate increased sharply at the near wall regions and both distributed more uniformly. The blade region in leading edge near suction side, trailing edge and volute tongue were the main regions to generate irreversible exergy loss. This research broadens a completely new view in evaluating energy loss and further optimizes pump using entropy production minimization.

Keywords: *entropy production, centrifugal pump, numerical simulation, energy loss evaluation*

0. Introduction

Rotating machinery like centrifugal pump and hydro turbine is very prevalent in many industries and other sectors. Research on its energy performance still draws more attention, however many studies in open literatures are still from traditional perspective of fluid dynamics. For example, the characteristic of pump used in turbine operating mode was numerically studied in Ref. [1]. The experimental research and CFD method are main techniques in measuring hydraulic performance of

[*]Corresponding authors, e-mail: zhyx@cup.edu.cn; houhucan@163.com;

the whole system or its component. Moreover, CFD method has been recognized by many researchers in the same field in simulating the inner field of centrifugal pumps [2]. Numerical simulations can provide accurate information in what one wants to know in detail and help to better understand the complex flow in impeller. However there still are some limitations in accurately locating where and how the hydraulic loss happens in one complex flow from traditional view. The traditional way is to calculate hydraulic loss indirectly from velocity and pressure fields and seems not intuitive.

Recently more and more studies in open literatures incline to build relationship between energy loss, such as hydraulic loss, and exergy loss due to irreversible entropy production [3-5]. Because any real physical process must have been accompanied with entropy production, the hydraulic loss in rotating machinery must obey basic laws and from the view of entropy production this part of energy can be captured by some way. Thus it can be explained and understood like this, this part of energy is dissipated in the flow process and becomes the energy loss, and then it is considered as source term subtracted from the governing equations without energy equation. At the first sight the source term representing hydraulic loss is simply disappeared, but actually the loss should be transformed into another kind of energy and can be captured by energy equation model in the form of entropy production energy. Therefore applying entropy production analysis method to evaluate energy loss is feasible and acceptable theoretically.

Zhang [6] uses the second law of thermodynamics to assure head loss coefficient by integration of volumetric entropy production rate field and proves entropy production analysis method is a feasible way. Herwig [7] et al offer a numerical simulation method to calculate roughness of arbitrary shape based on entropy theory and they prove that the dissipation model is applicative to laminar and turbulent flow. Kock and Herwig [8-9] define the local entropy production method and group them into four different mechanisms including dissipation in a mean and fluctuating velocity field and heat flux in a mean and fluctuating temperature field. Then the corresponding terms are incorporated into numerical simulations and regarded as a post process, which improves the practicability of local entropy production method.

In this work, the local entropy production analysis method was attempted firstly to apply in fluid machinery like centrifugal pump, which is rare to see in published literatures. Then it is adopted to apply to a centrifugal water pump and evaluate its energy loss, i.e., hydraulic loss. The steady numerical simulation based on Reynolds stress turbulent model was carried out to obtain the distribution of temperature, velocity and pressure fields and then after a post process, the entropy production compositions and distributions were calculated to evaluate energy loss of pump. As another form of energy conservation equation, the local entropy production analysis method is worth to draw more attention.

1. Theoretical analysis

1.1 Exergy analysis

Suppose there is an open steady flow system shown in Fig. 1, one single strand of fluid flows in and out the system. Provided the system boundary is adiabatic and ignore potential energy. The working fluid per unit mass brings energy of $h_1 + 0.5c_{f1}^2$ in from inlet and carries out energy of $h_2 + 0.5c_{f2}^2$ from outlet. During this process the working flow can also output internal power w_i, thus the system energy equation and exergy equation [10] can be given as eqs. (1) and (2). If the system is

only one flow device without power transportation, the terms w_i and e_{wi} should be zero, which is rightly suitable to the pipe flow for air and water appeared in the next study of this research. As for air flow, the entropy is calculated as follows.

$$h_1 + 0.5c_{f1}^2 = h_2 + 0.5c_{f2}^2 + w_i \quad (1)$$

$$\begin{aligned} i &= e_{h1} - e_{h2} + 0.5c_{f1}^2 - 0.5c_{f2}^2 - e_{wi} \\ &= h_1 - h_2 - T_r\left(s_1 - s_2\right) + 0.5c_{f1}^2 - 0.5c_{f2}^2 - e_{wi} \end{aligned} \quad (2)$$

$$s = c_p \ln T/T_r - R_g \ln p/p_r \quad (3)$$

In eq. (3), the reference temperature T_r and pressure p_r is chosen in inlet state. As for air flow at 300 K, T_r=300 K, p_r=101325 Pa, c_p=1006.43 J/(kg K) and R_g=287 J/(kg K).

Figure 1. Exergy equilibrium model of an open steady flow system

1.2 Entropy analysis

A real irreversible thermodynamic process always accompanies with irreversible loss. As for the turbulent flow in pump and due to the effect of fluid viscosity and Reynolds stress, the mechanical energy is inevitably transformed into internal energy. The energy loss, called hydraulic loss in pump, is generated by energy dissipation. However, such kind of energy dissipation is only one kind of energy conversion from exergy (available work) into anergy (unavailable work) from the perspective of the second law of thermodynamic. Rightly entropy is one perfect variable to measure exergy loss. Thus entropy can be used to measure mechanical energy loss, i.e., hydraulic loss in pump flow.

As a state variable in flow field, the specific entropy *s* has its own transportation equation for a single-phase incompressible flow, see for Spurk [11].

$$\rho\left(\frac{\partial s}{\partial t} + u\frac{\partial s}{\partial x} + v\frac{\partial s}{\partial y} + w\frac{\partial s}{\partial z}\right) = -\mathrm{div}\left(\frac{\bar{q}}{T}\right) + \frac{\Phi}{T} + \frac{\Phi_\Theta}{T^2} \quad (4)$$

In eq. (4) the last two terms represent mechanism for entropy production. The first means entropy production derived from viscous dissipation and the second term describes entropy production by heat transfer process for finite temperature gradient. These two terms are always positive.

In eq. (4) *s* is the only unknown variable, which is function of temperature and pressure for single phase flow. In addition, pressure, velocity and temperature field can be determined by the basic governing equations of mass, momentum and energy conservation. These three variables can be assured through a conventional numerical simulation by CFD. Hence theoretically *s* can be considered as a post process quantity which is determined by the flow field of temperature and pressure and it is no need to directly solve this transportation equation.

Because *s* is an instantaneous variable in eq. (4), like the conventional Reynolds averaged process, *s* also can be separated into two parts by extending the Reynolds averaged procedure to the entropy balance equation [12], namely the mean quantity part and the fluctuating part.

$$\rho\left(\frac{\partial \bar{s}}{\partial t} + \bar{u}\frac{\partial \bar{s}}{\partial x} + \bar{v}\frac{\partial \bar{s}}{\partial y} + \bar{w}\frac{\partial \bar{s}}{\partial z}\right) = \overline{\mathrm{div}\left(\frac{\bar{q}}{T}\right)} - \rho\left(\overline{\frac{\partial u's'}{\partial x}} + \overline{\frac{\partial v's'}{\partial y}} + \overline{\frac{\partial w's'}{\partial z}}\right) + \frac{\overline{\Phi}}{T} + \frac{\overline{\Phi_\Theta}}{T^2} \quad (5)$$

In eq. (5), $\overline{\Phi/T}$ is time averaged entropy production by dissipation and can be separated into two parts: one with mean and one with fluctuating terms [13].

$$\frac{\overline{\Phi}}{T} = S_{pro,\bar{D}} + S_{pro,D'} \quad (6)$$

$$S_{pro,\bar{D}}=\frac{\mu}{T}\left\{2\left[\left(\frac{\partial\bar{u}}{\partial x}\right)^2+\left(\frac{\partial\bar{v}}{\partial y}\right)^2+\left(\frac{\partial\bar{w}}{\partial z}\right)^2\right]+\left(\frac{\partial\bar{u}}{\partial y}+\frac{\partial\bar{v}}{\partial x}\right)^2+\left(\frac{\partial\bar{u}}{\partial z}+\frac{\partial\bar{w}}{\partial x}\right)^2+\left(\frac{\partial\bar{v}}{\partial z}+\frac{\partial\bar{w}}{\partial y}\right)^2\right\} \tag{7}$$

$$S_{pro,D'}=\frac{\mu}{T}\left\{2\left[\overline{\left(\frac{\partial u'}{\partial x}\right)^2}+\overline{\left(\frac{\partial v'}{\partial y}\right)^2}+\overline{\left(\frac{\partial w'}{\partial z}\right)^2}\right]+\overline{\left(\frac{\partial u'}{\partial y}+\frac{\partial v'}{\partial x}\right)^2}+\overline{\left(\frac{\partial u'}{\partial z}+\frac{\partial w'}{\partial x}\right)^2}+\overline{\left(\frac{\partial v'}{\partial z}+\frac{\partial w'}{\partial y}\right)^2}\right\} \tag{8}$$

In eq. (5), $\overline{\Phi_\Theta/T^2}$ is entropy production generated by heat transfer and it also can be separated into two parts, one with mean and one with fluctuating terms.

$$\overline{\frac{\Phi_\Theta}{T^2}}=S_{pro,\bar{C}}+S_{pro,C'} \tag{9}$$

$$S_{pro,\bar{C}}=\frac{\lambda}{\bar{T}^2}\left[\left(\frac{\partial\bar{T}}{\partial x}\right)^2+\left(\frac{\partial\bar{T}}{\partial y}\right)^2+\left(\frac{\partial\bar{T}}{\partial z}\right)^2\right] \tag{10}$$

$$S_{pro,C'}=\frac{\lambda}{\bar{T}^2}\left[\overline{\left(\frac{\partial T'}{\partial x}\right)^2}+\overline{\left(\frac{\partial T'}{\partial y}\right)^2}+\overline{\left(\frac{\partial T'}{\partial z}\right)^2}\right] \tag{11}$$

Consequently there appear four groups of entropy production terms in turbulent flow in eq. (5) called local entropy production rate. $S_{pro,\bar{D}}$ is local entropy production rate due to direct dissipation, $S_{pro,D'}$ is local entropy production rate due to turbulent dissipation, $S_{pro,\bar{C}}$ is local entropy production rate by mean temperature gradients and $S_{pro,C'}$ is local entropy production rate by fluctuating temperature gradients. $S_{pro,\bar{D}}$ and $S_{pro,\bar{C}}$ can be directly calculated using the known field quantities of velocity and temperature from CFD. But $S_{pro,D'}$ and $S_{pro,C'}$ are still unknown which are believed to be related with some turbulent model. Kock and Herwig [8, 9] proposed that these two terms can relate to turbulent dissipation rate ε and mean temperature $\bar{T}$ by all turbulent models, then they changed to the following forms.

$$S_{pro,D'}=\frac{\rho\varepsilon}{\bar{T}} \tag{12}$$

$$S_{pro,C'}=\frac{\alpha_t}{\alpha}S_{pro,\bar{C}} \tag{13}$$

According to Duan [14] $S_{pro,\bar{C}}$ and $S_{pro,C'}$ can be united into one term.

$$S_{pro,C}=\frac{\lambda_{eff}}{\bar{T}^2}\left[\left(\frac{\partial\bar{T}}{\partial x}\right)^2+\left(\frac{\partial\bar{T}}{\partial y}\right)^2+\left(\frac{\partial\bar{T}}{\partial z}\right)^2\right] \tag{14}$$

$$\lambda_{eff}=\lambda+\lambda_t \tag{15}$$

$$\lambda_t=\frac{c_p\mu_t}{Pr_t} \tag{16}$$

Until now, the four local entropy production terms can be calculated through eqs. (7), (12) and (14). Then the total entropy production rate of computational domain can be calculated by volume integration of each local entropy production term.

$$\Delta S_{pro,\bar{D}}=\int_V S_{pro,\bar{D}}\,dV \tag{17}$$

$$\Delta S_{pro,D'}=\int_V S_{pro,D}\,dV \tag{18}$$

$$\Delta S_{pro,C}=\int_V S_{pro,C}\,dV \tag{19}$$

The conventional CFD numerical solution can give a relatively accurate result of the flow in far-off the walls. The flow close to a wall is always related by the famous law of wall function that

states a logarithmic velocity profile in the near wall region. In these regions due to the extremely steep gradient of mean velocity and temperature, the local entropy production rate appears peak value and without extra consideration the volume entropy production rate calculated by Reynolds stress turbulent model will lead to unacceptable error. Therefore the entropy production rate in near walls should be calculated separately. Inspired by Zhang [15], the entropy production rate near wall regions, call wall entropy production rate, can be calculated by eq. (20) and thus the integral range of local entropy production terms by eq. (17) will not include the near wall regions while they are still referred by the original formulas.

$$\Delta S_{pro,W} = \int_s \frac{\overrightarrow{\tau_w} \cdot \overrightarrow{v_p}}{\overline{T}} dS \tag{20}$$

In this equation $\overrightarrow{\tau_w}$ is wall shear stress vector, $\overrightarrow{v_p}$ is the velocity vector at the grid center of the first boundary layer in immediate vicinity of walls. Then the total entropy production ΔS_{pro} of a system can be summarized in eq. (21). The exergy loss I_{pro} caused by entropy production reads in eq. (22).

$$\Delta S_{pro} = \Delta S_{pro,\overline{D}} + \Delta S_{pro,D'} + \Delta S_{pro,C} + \Delta S_{pro,W} \tag{21}$$

$$I_{pro} = \sum_i I_i = \sum_i \left(T_r \Delta S_{pro,i} \right) \quad i = \overline{D}, D', C, W \tag{22}$$

2. Numerical simulation

2.1 Governing equations

During the numerical simulation, water is selected as the working fluid and the simulation is performed based on the following assumptions: the process is in steady state; the fluid is incompressible; the flow is turbulent; the viscous dissipation is considered; the thermo physical properties of the working fluid are constant. Based on the assumptions above, the basic governing equations are as follows.

Continuity equation:
$$\frac{\partial u_i}{\partial x_i} = 0 \tag{23}$$

Momentum equation:
$$\rho \frac{\partial}{\partial x_j}\left(u_j u_i\right) = \frac{\partial}{\partial x_j}\left[-p\delta_{ij} + \mu\left(\frac{\partial u_i}{\partial x_j} + \frac{\partial u_j}{\partial x_i} \right) \right] \tag{24}$$

Energy equation:
$$\rho \frac{\partial}{\partial x_j}\left(u_j T\right) = \frac{\lambda}{c_p}\frac{\partial^2 T}{\partial x_j^2} + \mu\left(\frac{\partial u_i}{\partial x_j} + \frac{\partial u_j}{\partial x_i} \right)\frac{\partial u_i}{\partial x_j} \tag{25}$$

δ_{ij} is Kronecker delta. The second term on the right hand side of eq. (24) and eq. (25) is viscous dissipation term.

Applying the Reynolds averaged process on eq. (24), the RANS equations can be rewritten as follows.

$$\rho \overline{u}_j \frac{\partial \overline{u}_i}{\partial x_j} = \frac{\partial}{\partial x_j}\left[-\overline{p}\delta_{ij} + \mu\left(\frac{\partial \overline{u}_i}{\partial x_j} + \frac{\partial \overline{u}_j}{\partial x_i} \right) - \rho \overline{u_i' u_j'} \right] \tag{26}$$

And the Reynolds stress transport equation is express as follows.

$$\frac{\partial}{\partial t}\left(\rho \overline{u_i' u_j'} \right) + \frac{\partial}{\partial x_k}\left(\rho u_k \overline{u_i' u_j'} \right) = D_{T,ij} + D_{L,ij} + P_{ij} + G_{ij} + \phi_{ij} + \varepsilon_{ij} + F_{ij} + S_{ij} \tag{27}$$

Where the detailed parameters can be seen in Ref. [14].

2.2 Geometry model and grid generation

One IS series centrifugal pump is considered as research object and the model of the pump IS 150-125-250 is shown in Fig. 2. The design parameters for this pump are the design flow rate of 200

m^3/h, the head of 20 m and the hydraulic efficiency of 0.95.

As the geometrical structure of pump model was given, the computational domains could be generated mainly including four parts inlet duct, impeller, volute and outlet duct shown in Fig. 3(a). In Fig. 3(b), the structured hexahedral grid was compelled in inlet and outlet duct by ICEM and five layers grid of boundary layer were fixed in the near-wall region with the first layer height of 0.5 mm and the growth rate of 1.1. Considering the complexity of volute geometry and skewness of impeller, the unstructured tetrahedral grid was used by ANSYS-Meshing. The mesh refinement technique was applied to the blade surfaces and y^+ around the wall was controlled less than 200 meeting the requirement of Reynolds stress turbulent model during calculation. Then grid independence has been investigated for reducing of computational time and improving reliability of calculation accuracy at the design flow condition. As shown in tab. 1 the pump head H and efficiency η are chosen as the evaluation parameters for the effect of mesh size on final solution. After contrastive analysis of different sets of meshes, the H and η change very little with grid number up to 1.77 million cells with the error only 0.52% for H and 0.44% for η. Therefore the mesh of 1.77 million cells is used for next simulation.

Table 1. Hydraulic performance of pump calculated by different mesh numbers

Mesh number ($/10^6$)	Head H (m)	Error (%)	Efficiency η (%)	Error (%)
0.78	21.44		84.13	
1.24	20.62	3.98	82.57	1.56
1.77	20.32	1.46	81.65	0.92
2.36	20.21	0.52	81.21	0.44

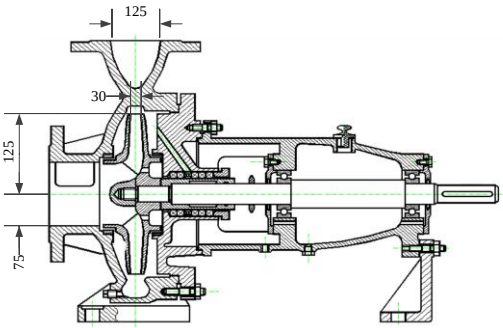

Figure 2. Pump geometrical structure

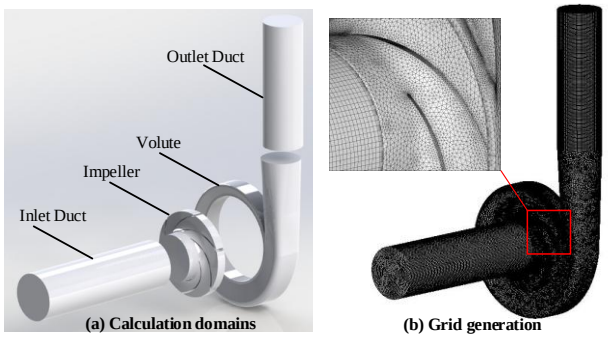

Figure 3. Computational domains and grid

2.3 Flow solver and boundary conditions

The solver of commercial software ANSYS Fluent 14.0 was used to calculate flow field. The Reynolds stress turbulent model and SIMPLEC algorithm were applied to solve RANS equations. Velocity inlet was applied for inlet boundary by assuming that velocity at inlet cross-section is uniform. The turbulent intensity and hydraulic diameter are 3% and 150 mm respectively. Outflow was used for outlet boundary. The non-slip condition was given at solid walls. The Multiple Reference Frame (MRF) model was applied to take into account the interaction between stationary volute and rotating impeller with interface pairs. The standard wall function based on the logarithmic law has been used. PRESTO! Scheme is used for pressure term and second order upwind discretization scheme is used for convection terms. The convergence criterion of numerical simulation was set as a residual of 10^{-4}.

3. Results and discussions

3.1 Validation of pump hydraulic performance

The pump model researched is one IS series and then optimized by BVF diagnosis method in Ref. [16-17]. As shown in Fig. 4, the performance comparison between numerical simulation results based on Reynolds stress turbulent model and experimental data is carried out. Under the flow rate ranging from 160 m^3/h to 240 m^3/h, the head vs. flow rate curve is a little higher than experimental. The maximum absolute deviation is only 0.33 m and the maximum relative error is 1.65%. The efficiency in Fig. 4 is calculated by considering the leakage loss and mechanical loss, which are calculated by empirical formula in Ref. [18] based on pump specific speed and they are 0.974 and 0.952 at the design flow condition respectively. Generally the whole pump performance is improved and moreover the numerical simulation results agree well with the experimental data, which indicates that the selected pump is proper and numerical methods are no problem.

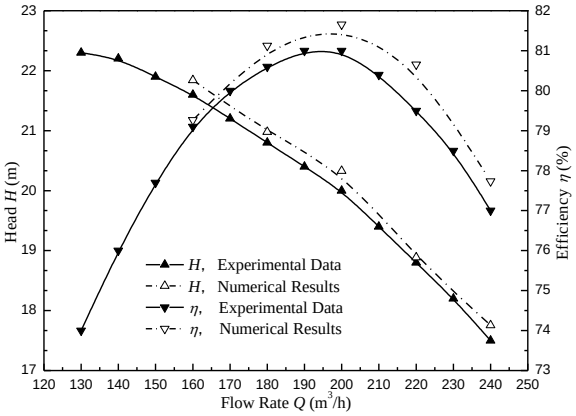

Figure 4. Hydraulic performance curves of pump

3.2 Energy loss analysis by local entropy production analysis method

As shown in Fig. 5, the energy loss by local entropy production method for each component is presented. The energy loss by entropy production method near the design flow condition is the minimum. At off-conditions especially the large flow rates, the energy loss increases sharply. The energy loss for the whole flow passage drops slowly from 160 m^3/h, reaches to the trough from 180 m^3/h to 200 m^3/h and then rapidly increases at 240 m^3/h. Such variation trend is in accord with efficiency vs. flow rate curve that the pump performance is nearing the optimal from 180 m^3/h to 200 m^3/h. Meanwhile the energy loss in volute is larger than that in impeller, which indicates that the volute is not very good to match the impeller. The energy loss in impeller is almost the same level at different flow conditions and generally declines.

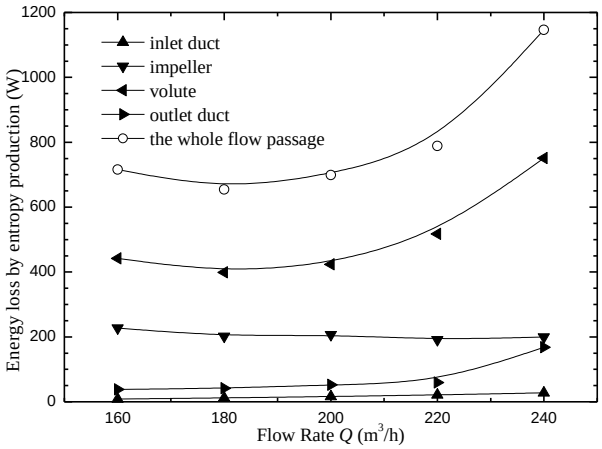

Figure 5. Energy losses for each component of pump

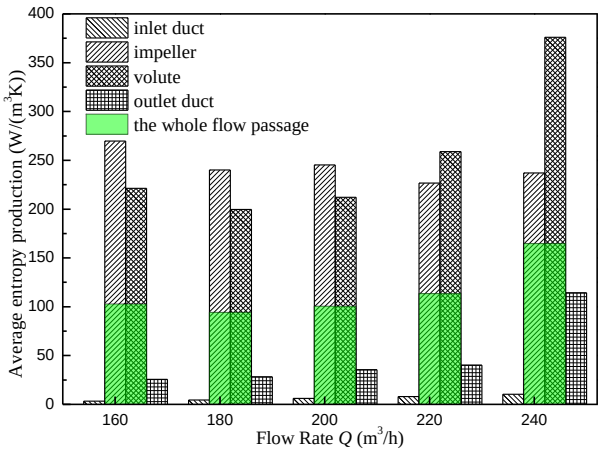

Figure 6. Average entropy productions for each component of pump

In order to obtain quite good hydraulic performance for a centrifugal pump, the components like impeller and volute must be designed as a good match. Good match will reduce hydraulic loss greatly. Fig. 6 and tab. 2 present the average entropy production rate for each component of pump and its

proportion in total value. Fig. 6 reads that with the flow rate increasing from 160 m^3/h to 240 m^3/h, the average entropy production rate in impeller and volute possesses the large part and they are both larger than that in the whole flow passage as shown in green domains. The average entropy production rate in impeller is greater than that in volute at the small flow rate range while it is completely opposite at the large flow rate range. On the whole the average entropy production rate in impeller keeps in the same value level but still decreases very slowly and as for volute it decreases first and then increases fast. The other components inlet duct and outlet duct are increasing all along. Therefore in the pump flow for water, the impeller and volute are the main domains to generate irreversible energy loss.

Table 2. Proportions in total entropy production for each component of pump (%)

Component	Flow rate Q (m^3/h)				
	160	180	200	220	240
inlet duct	1.23	1.85	2.33	2.70	2.37
impeller	31.75	30.89	29.56	24.22	17.42
volute	61.74	60.92	60.62	65.59	65.54
outlet duct	5.29	6.34	7.48	7.49	14.67
Total	100	100	100	100	100

Tab. 2 lists the entropy production proportion for each component of pump. It is more obvious that the entropy production in impeller and volute account for 30% and 60% in total value respectively. Although the average entropy production for impeller and volute are almost in the same level, the proportion in volute is more or less twice of that in impeller because the volume of volute is much bigger than that of impeller.

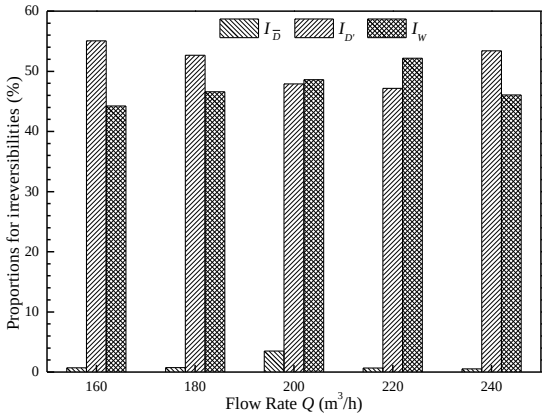

Figure 7. Various entropy productions due to irreversibility of pump

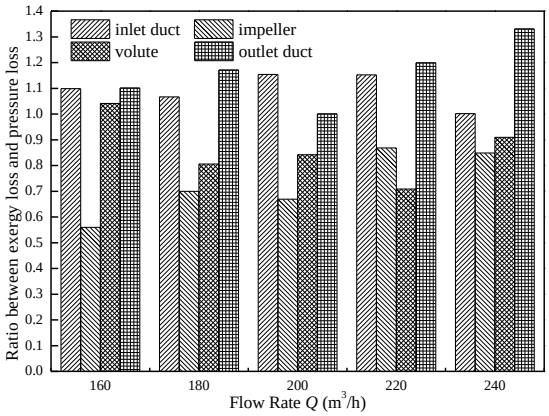

Figure 8. Ratio between energy loss calculated by entropy production and pressure drop

In order to better understand various kinds of entropy productions for the whole entropy production, Fig. 7 presents the proportions for each kind of entropy. Obviously the proportion of entropy production caused by direct dissipation is quite small and the value is ranging from 0.54% to 3.48%. Therefore this kind of entropy production also can be ignored in pump. Furthermore, the entropy production caused by turbulent dissipation and wall viscous friction account for the great part in the whole entropy production and they are 47%~55% and 44%~52% respectively under the research flow rate range. Thus the irreversible energy loss in water pump flow is mainly caused by turbulent dissipation and wall friction. At the flow rate of 200m^3/h, the entropy production caused by turbulent dissipation and wall friction takes up 47.91% and 48.61% respectively. With the flow rate increasing from 160 m^3/h to 240 m^3/h, turbulent entropy production decreases first and then increases

greatly while wall friction entropy increases evidently all along. But at the flow rate of 240 m^3/h, wall friction entropy production is sharply reduced.

3.3 Comparison between entropy production energy loss and pressure energy loss

Generally the total pressure increase between inlet and outlet of impeller is used to measure the power capacity and in order to assess and verify the feasibility of the second law of thermodynamics in analyzing pump energy consumptions; the pressure drop for each component can be transferred to energy loss according to eq. (28). As for impeller, the energy loss should be the total input energy shaft power subtracting the total pressure increase for working water.

$$I_{\mathrm{i}} = \int_{\mathrm{in}} p_{\mathrm{tot}} \mathrm{d}q_v - \int_{\mathrm{out}} p_{\mathrm{tot}} \mathrm{d}q_v \quad \text{i=inlet duct, volute, outlet duct} \tag{28}$$

In the equation above p_{tot} is the total pressure at the inlet and outlet section and q_{v} is the volume flow rate.

As shown in Fig. 8, different methods including local entropy production and pressure drop are used to calculate energy loss and the ratio between them are listed. Generally the energy loss by entropy production method agrees well with that by pressure drop. Taking the computational domains such as inlet duct and outlet duct for example, the ratio ranges from 1.00 to 1.15 for inlet duct and from 1.00 to 1.19 for outlet duct, and the average value are 1.09 and 1.16. Obviously the average deviation is 9% and 16%, which is acceptable in engineering application. The deviation for outlet duct is bigger than that for inlet duct. As for impeller and volute the ration ranges from 0.56 to 0.87 and from 0.70 to 1.04, respectively. The average ratio value is only 0.73 and 0.86. Considering the highly accurate application of this method on pipe flow, it is believed that the deviation here is caused by the high rotatibility and curvature of impeller and volute. Although the local entropy production method is feasible to assess the irreversible energy loss for pump water flow but needs further study. The next work will be focus on how curvature and rotation influence the result and proposing the correction schemes.

3.4 The distribution of entropy production in pump water flow

Through the analysis of entropy production above, the entropy production by direct dissipation and temperature gradient can be ignored in pump water flow, thus the entropy production caused by turbulent dissipation and wall friction is chosen to show its distribution in pump. Fig. 9 shows the distribution of volumetric entropy production rate due to turbulent dissipation and velocity for inlet duct and outlet duct under the flow rate of 200 m^3/h. From Fig. 9 it can be seen that as for the inlet duct and outlet duct, the volumetric entropy production rate distributes quite uniformly and the value is quite small in the core flow, however they both increase sharply in the near wall regions. This tells that the entropy production by turbulent dissipation has a strong wall effect, i.e., it sharply increases in the near wall regions. Also the volumetric entropy production rate in outlet duct is quite higher than that in inlet duct. It can be explained that influenced by the impeller and volute, the flow in outlet duct is more disorder with higher velocity field compared with that in inlet duct.

As shown in Fig. 10, the distribution of volumetric entropy production rate and turbulent kinetic energy dissipation rate at the mid-span of impeller is extraordinarily similar. Almost at every leading edge of blades, the volumetric entropy production rate increases sharply, thus the blade leading edge is the main region generating irreversible energy loss. And combining the Fig. 11, it is quite obvious that the volumetric entropy production rate at the suction side is higher than that at the pressure side and

the region near the leading edge appears the peak value for the incidence flow. The distribution is very uniform at pressure side while there is one peak region at the suction side. From the distribution of relative velocity at the mid-span of impeller, it reads that the flow at suction side is more disorder than that at pressure and generally the flow is quite uniform which indicates that the impeller after optimization has a good hydraulic performance.

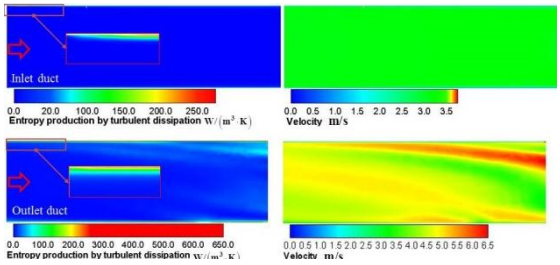

Figure 9. Distribution of turbulent production and velocity of inlet duct and outlet duct

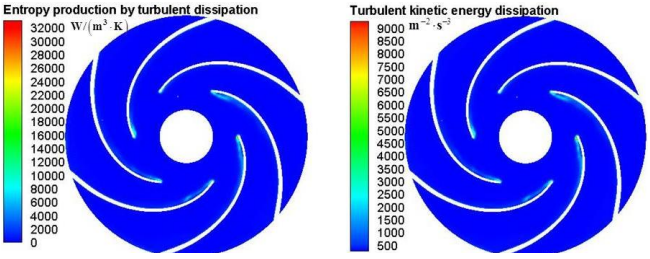

Figure 10. Distribution of volumetric entropy production rate and turbulent kinetic energy dissipation at mid-span of impeller

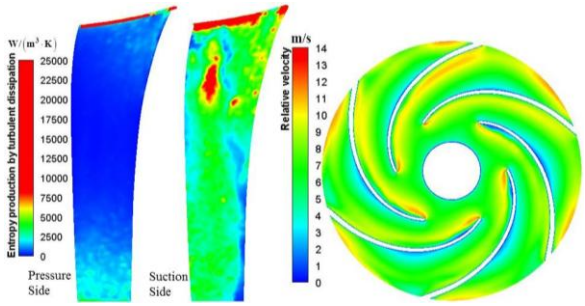

Figure 11. Distribution of volumetric entropy production rate at blades and relative velocity at mid-span of impeller

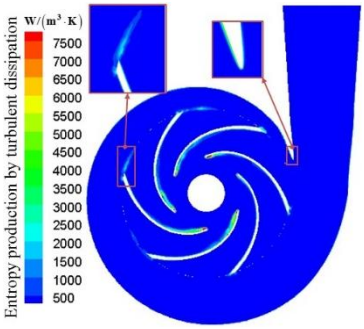

Figure 12. Distribution of volumetric entropy production rate at mid-span of volute

Fig. 12 presents the volumetric entropy production distribution at the mid-span of volute. Generally the value of volumetric entropy production is quite small in most of the volute regions. However there appear some peak regions at the interface between impeller and volute, which is rightly at the position of blade trailing edge. Influenced by the blade rotation, the outlet of impeller always induces the wake flow and brings about flow separation. Thus the volumetric entropy production in the trailing edge is obviously high but less than that in the leading edge. Meanwhile at the tongue of volute, there also appears obvious volumetric entropy production, indicating that the tongue is also one major place to produce irreversible energy loss.

4. Conclusions

Inspired by the second law of thermodynamics, the local entropy production method has been introduced into pump flow and some conclusions can be drawn as follows.

(1)The direct dissipation entropy production only takes up very small part and entropy production by turbulent dissipation and wall viscous friction are the major factor to generate energy loss. At the flow rate of 200 m^3/h, the entropy production caused by turbulent dissipation and wall friction takes up 47.91% and 48.61% respectively.

(2) The result for inlet duct and outlet duct agrees well between two calculation ways, but large discrepancy is still existing in impeller and volute. It is the high rotatibility and curvature for impeller and volute leading to the big deviation for pump water flow. The next work will be focus on how

curvature and rotation influence the result and proposing the correction schemes.

(3)The volumetric entropy production rate distributes quite uniformly to turbulent dissipation rate and it increases sharply in the near wall regions. The leading edge near suction side, the trailing edge and the volute tongue are the main regions to generate entropy production while it is quite obvious in the leading edge regions.

Acknowledgement

This research was supported by Science Foundation of China University of Petroleum, Beijing (No.2462015YQ0411).

Nomenclature

c_f – fluid velocity, [ms^{-1}]
c_p – specific heat capacity, [Jkg^{-1}K^{-1}]
d – diameter, [m]
e – specific exergy, [Jkg^{-1}]
e_h – specific enthalpy exergy, [Jkg^{-1}]
e_{wi} – specific output power exergy, [Jkg^{-1}]
h – specific enthalpy, [Jkg^{-1}]
h_f – linear loss, [W]
i – specific exergy loss, [Jkg^{-1}]
I_e – exergy loss by exergy equation, [W]
I_p – energy loss by Bernoulli, [W]
I_{pro} – exergy loss by entropy equation, [W]
k – turbulent kinetic energy, [m^{2}s^{-2}]
l – length, [m]
p – pressure, [P$_a$]
p_{tot} – total pressure, [P$_a$]
p_r – Prandtl number, [-]
$\vec{q}$ – heat flux density vector, [Wm^2]
q_m – mass flow, [kgs^{-1}]
q_v – volumetric flow, [m^{-3}s^{-1}]
R_e – Reynolds number, [-]
R_g – gas constant, [Jkg^{-1}K^{-1}]
s – specific entropy, [Jkg^{-1}K^{-1}]
S – surface area, [m^2]
S_{pro} – entropy production rate, [Wm^{-3}K^{-1}]
ΔS – volumetric entropy production, [WK^{-1}]
t – time, [s]
T – temperature, [K]
u v w – velocity in x, y, z directions, [ms^{-1}]
V – volume, [m^3]
$\vec{V}_p$ – wall velocity vector, [ms^{-1}]
w_i – specific output power, [Jkg^{-1}]
x, y, z – coordinate in x, y, z directions, [m]

Greek symbols

α – thermal diffusivity, [m^{2}s^{-1}]
α_h – energy loss ratio, [-]
δ_{ij} – Kronecker delta
ε – turbulent dissipation rate, [Wkg^{-1}]
λ – thermal conductivity, [Wm^{-1}K^{-1}]
λ_{eff} – effective thermal conductivity, [Wm^{-1}K^{-1}]
μ – molecular viscosity, [kgm^{-1}s^{-1}]
ρ – density, [kgm^{-3}]
τ – shear stress, [Wm^{-1}s^{-2}]
Φ – viscous dissipation term, [Wm^{-3}]
Φ_Θ – entropy production term, [WKm^{-3}]

Subscripts & Superscripts

$()_1$ – inlet position
$()_2$ – outlet position
$()_C$ – heat transfer
$()_D$ – about viscous dissipation
$()_r$ – ambient state
$()_t$ – about turbulence flow
$\overline{()}$ – mean component
$()'$ – fluctuating component

References

[1] Bogdanović-Jovanović, Jasmina B., et al, Pumps used as turbines power recovery, energy efficiency, CFD analysis, *Thermal Science, 18* (2014), 3, pp. 1029-1040.
[2] Zhang, Desheng, et al, Numerical investigation of blade dynamic characteristics in an axial flow pump, *Thermal Science, 17* (2013), 5, pp. 1511-1514.
[3] Mahian, Omid, et al, Design of a vertical annulus with MHD flow using entropy generation analysis, *Thermal Science, 17* (2013), 4, pp. 1013-1022.

[4] Malvandi, Amir, et al, Series solution of entropy generation toward an isothermal flat plate, *Thermal Science, 16* (2012), 5, pp. 1289-1295.
[5] Atashafrooz, Meysam, Nassab Abdolreza Seyyed Gandjalikhan, and Babak Amir Ansari, Numerical investigation of entropy generation in laminar forced convection flow over inclined backward and forward facing steps in a duct under bleeding condition, *Thermal Science, 18* (2014), 2, pp. 479-492.
[6] Zhang, H-C., B. Schmandt, and H. Herwig, Determination of loss coefficients for micro-flow devices: A method based on the second law analysis (SLA), *ASME 2009 Second International Conference on Micro/Nanoscale Heat and Mass Transfer*, American Society of Mechanical Engineers, 2009.
[7] Herwig, H., D. Gloss, and T. Wenterodt, A new approach to understanding and modelling the influence of wall roughness on friction factors for pipe and channel flows, *Journal of Fluid Mechanics, 613* (2008), pp. 35-53.
[8] Kock, Fabian, and Heinz Herwig, Entropy production calculation for turbulent shear flows and their implementation in CFD codes, *International Journal of Heat and Fluid Flow, 26* (2005), 4, pp. 672-680.
[9] Kock, Fabian, and Heinz Herwig, Local entropy production in turbulent shear flows: a high-Reynolds number model with wall functions, *International Journal of Heat and Mass Transfer, 47* (2004), 10, pp. 2205-2215.
[10] Shen Weidao, Jiang Zhimin, Tong Jungeng, *Engineering Thermodynamics*, Higher Education Press, 3rd ed. Beijing, China, 2001. (In Chinese)
[11] Förste J. Spurk, JH, Strömungslehre, 1989.
[12] Kock, Fabian, Bestimmung der lokalen Entropieproduktion in turbulenten Strömungen und deren Nutzung zur Bewertung konvektiver Transportprozesse, *Shaker*, 2003.
[13] Herwig, H., and F. Kock, Direct and indirect methods of calculating entropy generation rates in turbulent convective heat transfer problems, *Heat and mass transfer, 43* (2007), 3, pp. 207-215.
[14] Duan Lu, Wu Xiaolin, and Ji Zhongli, Application of entropy generation method for analyzing energy loss of cyclone separator, *CIESC Journal, 65* (2014), 2, pp. 583-592. (In Chinese)
[15] Xiaomin, Zhang Xiang Wang Yang Xu, and Wang Hongyu. Energy conversion characteristic within impeller of low specific speed centrifugal pump, *Transactions of the Chinese Society for Agricultural Machinery 7* (2011), pp. 016. (In Chinese)
[16] Zhou, Xin, et al. The Impeller Improvement of the Centrifugal Pump Based on BVF Diagnostic Method, *Advances in Mechanical Engineering, 6* (2014), pp. 464363, DOI No. 10.1155.
[17] Zhou, Xin, et al, The Optimal Hydraulic Design of Centrifugal Impeller Using Genetic Algorithm with BVF, *International Journal of Rotating Machinery, 2014* (2014), DOI No.10.1155.
[18] Li Wenguang, Comparisons among several empirical formula of hydraulic efficiency, *Mechanical and electrical technology, 2* (1999), pp. 1-4. (In Chinese)